Graph-Based Analysis of Ethylene Glycol Decomposition on a Palladium Cluster

Remedios Cortese,[†] Roberto Schimmenti,[†] Francesco Ferrante,[†] Antonio Prestianni,[†] Donato Decarolis,[‡,§] and Dario Duca*[,†]

[†]Dipartimento di Fisica e Chimica, Universitàdegli Studi di Palermo, Viale delle Scienze Ed. 17, 90128 Palermo, Italy

[‡]Department of Chemistry University College of London, 20 Gordon Street, London, WC1H0AJ, U.K.

[§]Research Complex at Harwell (RCaH), Harwell, Didcot, Oxfordshire OX11 0FA, U.K.

* Supporting Information

ABSTRACT: The ethylene glycol, CH_2OH-CH_2OH, decomposition mechanism, occurring on a subnanometric palladium cluster shaped by 12 atoms, was investigated by means of density functional theory. Different reaction routes were identified leading to H_2 and CO. The whole reaction network was analyzed, framing the results within the graph theory. The possible decomposition pathways were discussed and compared, allowing one to draw a whole picture of all the parallel, possibly competitive, routes that starting from CH_2OH-CH_2OH originate H_2 and CO.

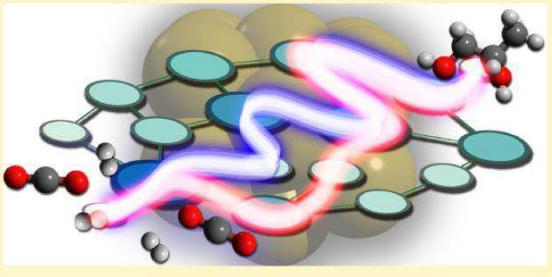

24, how

INTRODUCTION

Substrates recognizable as sustainable source of carbon and deriving from biomass raw materials have attracted in the past few years the attention of the scientific community. The interest was determined also thanks to the possibility to produce both environment-friendly hydrogen as well as chemicals of potential interest.[1−4] Generally, biomass-based feedstocks contain large amount of oxygenates, and these compounds mainly steer the reactivity of these processable materials. Studies on biomass conversion, demonstrated the efficacy of Pt- and Pd-supported catalysts, in the reforming processes hence in the consequent production of hydrogen.[5−7] Generation of H_2 from oxygenates proceeds through a combination of C−C bond scissions and dehydrogenation reactions to form hydrogen and carbon monoxide on the catalyst surface. The total amount of obtainable hydrogen is generally increased, coupling the reforming with the water gas shift reaction.

In order to maximize the production of H_2, the control of C−C bond cleavage is highly advantageous. This means that all the side reactions deriving from the C−O bond scission have to be suppressed to avoid alkane formation while dehydrogenation and decarbonylation should be promoted.[8,9] Various exper-imental and theoretical studies concerning the decomposition of alcohols and polyols[10] on Pd surfaces are reported in the literature.[7,11−19] As an example, Shekar and Barteau found that ethanol decomposes on both Pd(111) and (110) surfaces via dehydrogenation and decarbonylation steps, without any evidence of C−O scissions.[20] Alcohol decomposition on the Pt-group metals was believed to start by the O−H bond breaking, which would form an alkoxide intermediate.[21] However, according to more recent studies, the favored cleavage should be that involving the C−H bond.[22] In agreement with these experimental evidence, Li et al.,[23] investigating the ethanol decomposition on Pd(111) by means of periodic DFT calculations, found that the mechanism involving a C−H breaking as first stage should be preferred while decarbonylation would seem to be favored if compared to C−O bond breaking.

Yudanov and co-workers also focused on C−O bond cleavage on Pd nanoparticles, identifying it as a slow side process in the decomposition of methanol.[24] Sutton and Vlachos furthermore suggested, according to the results of their periodic DFT studies, that ethanol activation is remarkably consistent on metal surfaces, the initial step being either an O−H breaking (on Co, Ni, Rh, and Ru surfaces) or a C−H scission (on Pd and Pt surfaces). The initial activation is then followed by a series of relatively facile dehydrogenation reactions until C−C cracking occurs. The more oxophilic is the metal (e.g., Co and Ru), the more ethane is produced, but it is likely only a minor product.[25]

Although important advances in understanding the chemistry of several biomass-model molecules on idealized metal surfaces were made, the impact of low coordinated sites[26,27] and of characteristic geometric and electronic features caused by the subnanometric sizes of the catalyst received little attention. Since these aspects could give rise to variations in the reaction mechanism, as reported by Mehmood et al.[28] in a study dealing with the methanol decomposition on small Pd clusters, it is very useful to rationalize the effect of the sizes of the catalyst

that indeed might result in different catalytic activities and selectivities.

In this study, in view of disclosing elementary processes involved in the reforming of light polyols, ethylene glycol (CH_2OH-CH_2OH) was selected as a polyfunctional oxygenated model species, and its decomposition on a subnanometric Pd cluster was investigated by means of DFT. Studies dealing with the reactivity of this molecule are of interest both to enhance practical goals of hydrogen and syngas production and to provide fundamental insights into the underlying competition among C−H, O−H, C−C, and C−O bond cleavages in polyols.

The size of the catalytic system above, involving a small Pd cluster and simple C_2 species, allowed one to explore by computational techniques almost all the reactive routes associated with the ethylene glycol decomposition. This determined the generation of a large grid of possible events, useful to deepen the energetic ordering of different reaction pathways that in principle would let to isolate the whole reaction mechanism, involving many and complexly tangled molecular events. So, to effectively analyze the decomposition path, it is necessary to accurately characterize not only the elementary steps involved in the reaction network but also their hypothetical sequences, in the large ensemble of their possible combinations. For this purpose, within a graph theory (GT) based approach, in this work, all the pathways starting from CH_2OH-CH_2OH and leading to CO and H_2 were analyzed so as to draw a picture of the competitive routes leading to hydrogen production on a subnanometric Pd cluster.

MODELS AND COMPUTATIONAL DETAILS

All the reported calculations were performed within the density functional theory employing the Gaussian09 code.[29] As exchange-correlation functional the M06L developed by Zhao et al.[30] was selected since it was explicitly parametrized to have good performance for both main-group elements and transition metal chemistry. For the Pd atom the cc-pVDZ-PP effective core potential joined with its associated basis set was employed, whereas for the H, C, O atoms, the DZVP2 one was selected.

It was already shown that the fragmentation of hydrogen on a subnanometric palladium cluster lowers the number of unpaired electron of the whole system,[31,32] therefore, since the number of hydrogen atoms residing on the cluster is variable depending on the progress of the decomposition reaction, the geometries of the reagent, intermediate, product and transition state (TS) species were optimized with three different spin multiplicities (three, five, and seven). The search of TSs was performed with the Berny algorithm and all the stationary points were characterized by inspecting the vibrational frequencies calculated within the harmonic approximation. All the energy values reported include the vibrational zero point contribution and, where adsorption energies are discussed, the BSSE correction according to the counterpoise method was always applied. Activation barrier for a given elementary step was finally calculated taking as reference state the intermediate species preceding the TS associated with the considered molecular event.

A Pd_{12} cluster was selected as the catalyst. This was obtained following a growing process applied to a Pd_9 cluster, which already was extensively studied with respect to its electronic, structural and catalytic features.[31,33−35] In details, to the Pd_9 cluster, characterized by D_{3h} symmetry and quintet multiplicity, were added three Pd atoms in the convex faces then reoptimized. The most stable form of the resulting Pd_{12} had geometrical properties sensibly changed with respect to those of the initial guess, showing D_{2d} symmetry and septet spin multiplicity. Pd_{12} has three nonequivalent sites, with six (6c), five (5c) and four (4c) nearest neighbors, respectively, in turn delineating two triangular shaped hollows, namely H1(5c,4c,6c) and H2(5c,6c,6c). The cluster structure and the nonequivalent sites are shown in Figure 1.

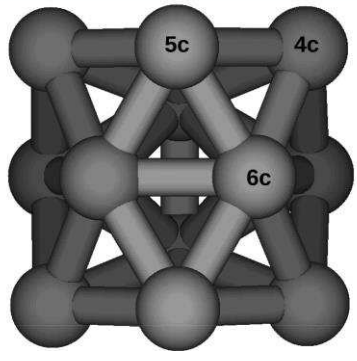

Figure 1. Pd_{12} cluster structure. The three nonequivalent sites having coordination number six (Pd^{6c}), five (Pd^{5c}), and four (Pd^{4c}) are pinpointed.

The whole reaction mechanism was framed and analyzed within a graph theory approach, so according to a GT formalism, nodes and edges of the graph were defined as the a given species to another one respectively. When the C−C bond is present, an intermediate species is named reporting first the node number that identifies its position in the graph, followed by the type of cleavage involved in its formation: C and O individuate C−H and O−H bond cleavage, respectively, whereas C−O does the same for the C−O bond cleavage. The node numbers are not connected with a decomposition process, as the former are randomly attributed. On the contrary, the sequence of capital letters, present in the acronym of a given intermediate species, identifies the number of elementary steps as well as the sequence of reactions necessary to produce that species. When the C−C bond is not present in the intermediate, the node number is followed by the produced fragments, closed in brackets and separated by a vertical bar.

It is important to underline that, molecular diffusion on the cluster has to occur for the fulfillment of some surface events. However, considering the very low activation barrier of these events with respect to the other elementary steps considered in this investigation, it was assumed that diffusion could take place freely, therefore, this was not included within the graph-based analysis. In details, the protocol followed for the reaction network analysis can be divided into three steps: (i) ab-initio calculation of the activation barriers and presieving of the possible molecular events, (ii) organization of the graph representing the final reaction network, and (iii) analysis of the possible pathways. Presieving of the molecular events was ruled by the assumption that one activation barrier related with other activation barriers and exceeding, one of the latter by ca. 30 kJ mol^{-1} correspond to a non competitive process. This assumption, which is justified considering the negative exponential dependence between the activation barrier and the kinetic constant of a given process, actually allowed us to exclude a lot of processes, enormously decreasing the involved intermediates and the molecular events leading from

connections number of the graph network. Once the events considered as feasible were isolated, the final graph was built. The analysis of the resulting network was performed considering that, as stated in the frame of the GT approach, a walk is an alternating succession of vertices and edges that starts with a vertex and ends with a vertex and a path is a walk in which no vertex occurs more than once. By use of a homemade python-based routine, forty-one simple paths of different length connecting the reactant and the product were found. The different lenght pathways found were ordered, taking into account the total energy content (TEC), defined as the summation of all the activation barriers involved in the development of a given route.

RESULTS AND DISCUSSION

The ethylene glycol decomposition mechanism on a subnanometric cluster was investigated, involving dehydrogenation and both C−C and C−O bond cleavages. Atomic hydrogens produced along with the dehydrogenation process were assumed to easily diffuse on the Pd_{12} cluster[31] hence every time a couple of chemisorbed hydrogen atoms was produced, it was removed from the metal cluster hypothesizing an easy desorption following a quick meeting of the same surface species. All the elementary reactions are in the following commented, highlighting which among the considered processes is or is not included in the final graph.

Devising the Graph: Description of Nodes and Edges. Adsorption of C_2 Species on Pd_{12}. Ethylene glycol adsorbed on the palladium cluster is identified by the N0 node of the graph. This is the source vertex used to evaluate all the simple paths, which characterize the whole ethylene glycol decomposition network. It is well-known that although twenty-seven ethylene glycol conformers exist the representative conformational space of the species is actually formed by just ten structures.[36] According to Prasanta et al.[37] the representative conformer ensemble ranges in-between an energy span of ca. 15 kJ mol^{-1}. In order to investigate the adsorption process of the $CH_2OH{-}CH_2OH$ molecules on the Pd_{12} cluster it was decided to consider only one conformer per each of the two limit staggered configurations (i.e. gauche and anti): the first ($C^g{}_2$) retains the intramolecular hydrogen bond while the other ($C^a{}_2$) not. For the sake of comparison, in vacuum, $C^g{}_2$ is 10.7 kJ mol^{-1} more stable than $C^a{}_2$, at the here level of theory while Prasanta et al., which employed the B3LYP exchange-correlation functional joined with the 6-311++G** basis set, calculated an energy difference for these two conformers (tGg′ and tTt in the cited work) of 9.0 kJ mol^{-1}.[37]

When approaching the cluster, the hydroxyl groups of the $CH_2OH{-}CH_2OH$ species might interact with one or more among three nonequivalent atop sites. Thus, to analyze the adsorption process, the $C^g{}_2$ species was placed with one −OH group pointing, in turn, to a 4c, 5c, and 6c site (see Figure 1). Among these configurations, that involving the 5c site resulted to be the most stable (those involving 4c and 6c sites actually were 5.7 and 32.9 kJ mol^{-1} higher in energy). Moreover, the adsorption energies of the $C^g{}_2$ and $C^a{}_2$ conformers on the 5c site were found to be −83.4 and −64.5 kJ mol^{-1}, respectively. The activation barrier for the conversion of the gauche conformer into the anti one was calculated, showing that the process on the Pd_{12} cluster requires at least 36.2 kJ mol^{-1} and that $C^a{}_2$ is 29.7 kJ mol^{-1} less stable than $C^g{}_2$, very likely because of the breaking of an intramolecular hydrogen bond in the former surface system. The activation barrier associated with the rotation on Pd_{12} hence is, in someway, affordable therefore it is possible to infer that the gauche conformer could transform into the anti one. This could be important because the possible occurrence of two different conformations would guarantee the proximity to the surface catalyst of different fragments of the same polyol. As a consequence, different molecular events might occur, starting from the two different geometrical arrangements.

$CH_2OH{-}CH_2OH$ Species: Node N0. Being aware that for highly hydrogen-saturated species the C−C bond scission is quite unlikely, this elementary step was not considered in the analysis of the initial stages of the reaction mechanism. Thus, due to the specific symmetry of $CH_2OH{-}CH_2OH$ just three bond breaking events involving C H, O H and C O have to be considered. All the intermediates formed in these processes are reported in Figure 2. It was found that the C−H

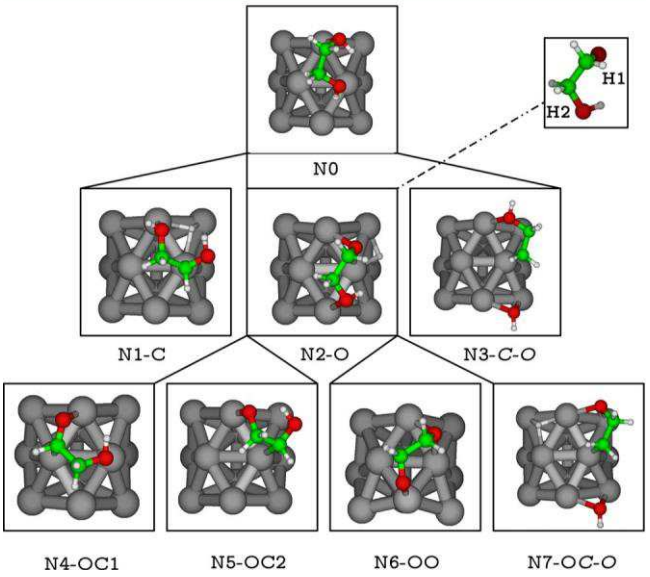

Figure 2. Intermediates formed in the first two hypothesized elementary steps of the catalyzed ethylene glycol decomposition. In the inset, on the right, the numbering associated with the H atoms related to the hydroxyl groups and belonging to the N2−O species is reported.

bond cleavage leading to the N1−C intermediate shows an activation barrier of 116.4 kJ mol^{-1}. The binding mode of the N1−C species with the Pd_{12} cluster is characterized by a multiple interaction determined by one $C{-}Pd^{6c}$ bond (2.06 Å), involving the dehydrogenated carbon, and one $O_H{-}Pd^{5c}$ bond (2.47 Å), formed by the hydroxyl group adjacent to the dehydrogenated carbon. The activation barrier for the O−H cleavage is 84.1 kJ mol^{-1}. The N2−O species shows a binding mode characterized by a concerted interaction occurring between the two oxygen atoms belonging to the C_2 molecule and the Pd cluster. The dehydrogenated oxygen is in a bridge position in-between a 5c and a 6c site ($O{-}Pd^{5c}$, 2.20 Å and $O{-}Pd^{6c}$, 2.27 Å), whereas the hydroxyl moiety interacts with a 5c site ($O_H{-}Pd^{5c}$, 2.43 Å). The C−O bond cleavage was showed to be not favored on Pd catalysts during the reforming of alcohols.[23] However, the activation barrier of the scission above was calculated, in order to rationalize eventual effects produced by the subnanometric sizes of the investigated particle catalyst. It was observed that also on a small Pd cluster the C−O rupture is highly demanding, being the energy

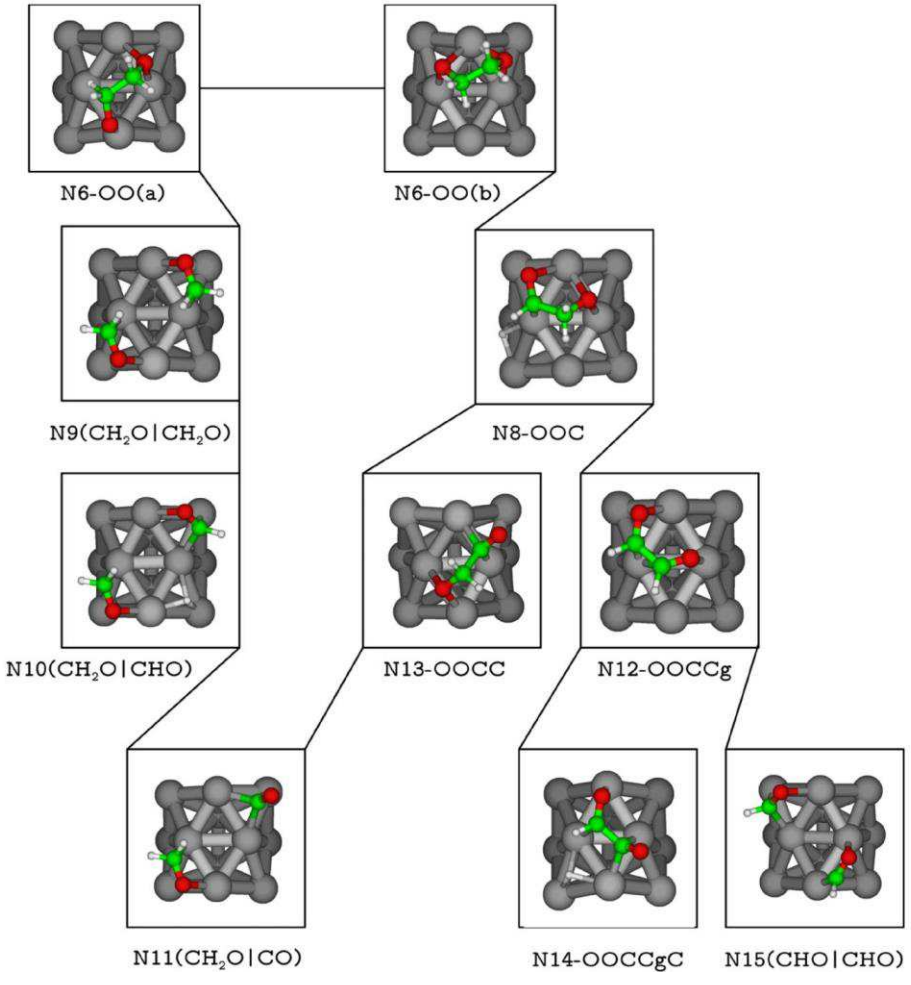

Figure 3. Schematic mechanism including the geometries of the intermediates deriving from the N6-OO species.

required to produce N3−C−O from N0 equal to 202.5 kJ mol^{-1}.

The results above confirm that dehydrogenation on palladium is more feasible than C−O cleavage, being the formation of alkoxide species favored. The results here reported are in line with previous experimental investigations, pointing out that for the transition metals belonging to the platinum-group the dissociative adsorption of alcohols leading to alkoxides is almost ubiquitous.[8,38] Nevertheless, for the sake of completeness, it should be recalled that in a previous theoretical study, dealing with decomposition of alcohols on Pd(111), it was reported that the first step, occurring along with reforming, is the cleavage of C−H, being the dehydrogenation of the hydroxyl fragment at all not competitive. In this study, Li et al.[23] for the ethanol C−H cleavage on a smooth Pd surface calculated an activation barrier value comparable to the one here reported i.e., 113.4 vs 116.4 kJ mol^{-1} whereas for the O−H breaking the two outcomes were very different. For the subnanometric cluster, the activation barrier is indeed sensibly lower i.e., 84.1 vs 160.2 kJ mol^{-1}. Despite the different substrates and theoretical approaches used to get them, it is reasonable to infer, considering the large disagreement found, that there could exist a connection between the subnanometric size of the metal particle and the easier hydroxyl dehydrogenation. In addition, a similar trend was also found in our recent work, dealing with Pd_6-catalyzed formic acid decomposition: in particular, it was demonstrated that the activation barrier for the O−H bond breaking is considerably lower on subnanometric clusters than on a Pd(111) smooth surface. On the contrary the activation barrier for the C−H bond cleavage was not affected by the size and shape of the catalyst.[39]

Comparing the activation barrier values characterizing the processes discussed above, it is possible to state that the steps leading to N1−C and N3−C−O are not competitive and have to be excluded from the reaction network landscape, leaving only the N2−O transformations as those to be further analyzed.

CH_2OCH_2OH Species: Node N2. Since N2−O shows two non equivalent C−H bonds, it is possible to hypothesize three dehydrogenation steps (C−H1, C−H2, O−H) as well as one C−O cleavage. Atom numbering and intermediates produced in these molecular events are reported in Figure 2. The process that involves the C−H1 bond cleavage has an activation barrier of 34.7 kJ mol^{-1} and produces a glycolaldehyde molecule, in the following identified as N4−OC1. This species interacts with the Pd_{12} cluster via the oxygen of the carbonyl moiety in a η_1 configuration. The occurrence of this binding mode (determining a calculated $O-Pd^{5c}$ distance equal to 2.17 Å) was already inferred by Mc Manus et al. who, analyzing a HREEL vibrational spectrum of glycolaldehyde adsorbed on Pd(111), reported that the ν(C O) stretching at 1715 cm^{-1} is slightly perturbed with respect to the one of the gaseous species.[7] There is convergence of results also regarding the reactivity of this species. In the study above it was, in fact, hypothesized that

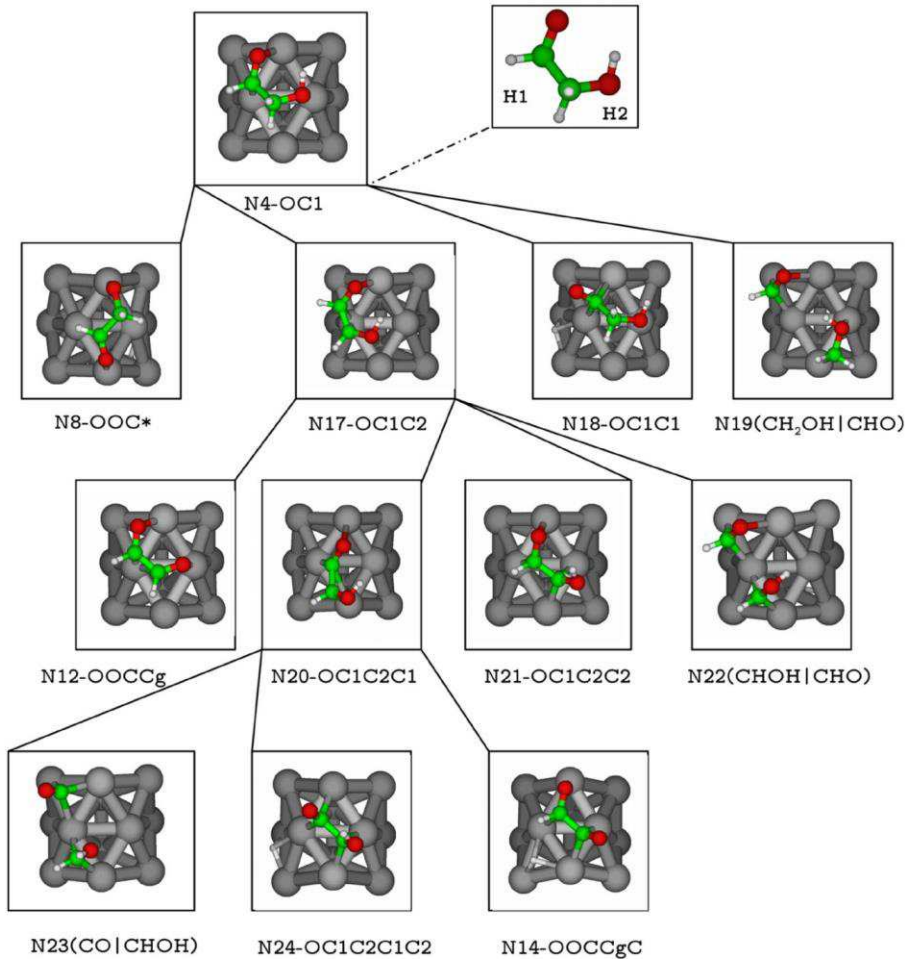

Figure 4. Schematic mechanism including the geometries of the intermediates deriving from the N4−OC1 species. Glycolaldehyde H atom numbering is reported in the inset.

the aldehydic species in order to react has to change the binding mode from η_1 to η_2. In agreement, this binding mode change was also observed, in the present work, for the transition state leading from N4−OC1 to N8−OOC*.

The activation barrier for the rupture of the C−H2 bond to form N5−OC2 resulted 99.2 kJ mol^{-1}; being the produced surface species chemisorbed via two stronger, C−Pd^{6c} (2.09 Å), O−Pd^{5c} (2.07 Å), and one weaker, O_H−Pd^{4c} (2.65 Å), interactions. The minimum amount of energy required to break the second O−H bond, originating the ethylenedioxy species, N6-OO, was equal to 75.6 kJ mol^{-1}. The binding mode of this dioxy-species involves interactions of both the oxygen atoms with the metallic cluster, one simple (O−Pd^{5c} 1.98 Å) and one having a bridge arrangement (O−Pd^{5c} 2.21 and O−Pd^{6c} 2.16 Å). This result is in agreement with Griffin et al., whose experimental studies on the reforming of CH_2OH−CH_2OH on Pd(111), suggested that this process is always characterized by the occurrence of surface species interacting by both the oxygen atoms.[40] For the sake of completeness, it should be said that the previous species, in accordance with the solely energetic criterion should have been excluded because of the limit of the 30 kJ mol^{-1}; however, considering the experimental findings above and the fact that the barrier exceeds of few kJ mol^{-1} the limit, the further decomposition of N6-OO was in any case investigated. The C−O cleavage of N2−O was also analyzed and the corresponding activation barrier, producing N7−OC−O, resulted 181.4 kJ mol^{-1}. In agreement with this energy value, the C−O rupture on Pd catalysts is always reported in the literature as highly unfavorable with respect of both the dehydrogenation and the C−C scission. As a consequence, the C−O rupture event was not further investigated to characterize the title reaction mechanism.

In summary, after the first dehydrogenation, which leads to the formation of an alkoxide species, the reaction mechanism shows a bifurcation, generating two branches that originate from ethylenedioxy (see Figure 3) and glycolaldehyde (see Figure 4) species. For sake of clarity, at first all the elementary steps deriving from the N6−OO species are, in the next eight sections, discussed and then, in the following, those related to the N4−OC1 intermediate.

CH_2OCH_2O Species: Node N6. Given the high symmetry of the ethylenedioxy molecule only the C−C and one C−H bond rupture were considered as possible. To break the C−H bond, however, a local diffusion step of N6−OO is necessary. This guarantees the right arrangement of the surface ethylenedioxy on the cluster, see the N6−OO(a) → N6−OO(b) step in Figure 3. Associated to the rearrangement an activation barrier of 17.8 kJ mol^{-1} was found. The corresponding TS shows a change in the binding mode of one of the two oxygens involved, that proceeds from a bridge surface interaction to an atop one. The right orientation could be actually reached also by rotating of 180° the OCCO torsion angle. This process, however, is well-known to be highly unfavored, since a strong

O−Pd interaction should be broken.[39,41] Once N6−OO reached by diffusion the correct arrangement to break the C−H bond, the minimum amount of energy necessary to cleave it and produce N8−OOC resulted 35.3 kJ mol^{-1}. This species interacts with the cluster via one O−Pd bridge bond (O−Pd^{5c} 2.25 Å, O−Pd^{6c} 2.13 Å), and one atop, C−Pd^{6c} bond (2.44 Å). Finally, the energy barrier to get two formaldehyde molecules, N9($CH_2O|CH_2O$), from N6-OO by means of a C−C cleavage, was found to be equal to 50.1 kJ mol^{-1}. According to the energetic range into which the activation barriers so far reported are included, all these processes were considered as feasible, and therefore further analyzed for unravel the title species reaction network.

$CHOCH_2O$ Species: Node N8. For the N8−OOC intermediate two nonequivalent C−H ruptures were evaluated. One of them led to glyoxal, N12−OOCCg, that showed a binding mode, involving four links with the Pd_{12} cluster. Among these, two were formed by both the carbon atoms with the same 6c palladium site (C−Pd^{6c} 2.34 and 2.45 Å) and two by both the oxygen atoms, which singly were connected to a 5c and a 6c site (O−Pd^{5c} 2.17 Å, O−Pd^{6c} 2.21 Å). This process was related to a small activation barrier, namely 16.6 kJ mol^{-1}. The other C−H cleavage produced N13−OOCC, an intermediate characterized by one Pd−O−Pd bridge (O−Pd^{5c} 2.16 Å, O−Pd^{6c} 2.20 Å) and one terminal CO moiety bridging two Pd atoms (C−Pd^{5c} 2.14 Å, C−Pd^{6c} 2.10 Å). The activation barrier for producing the N13−OOCC intermediate was equal to 32.3 kJ mol^{-1}. Further decompositions were investigated for both the intermediates formed through the two dehydrogen-ations just discussed.

CH_2O + CH_2O Fragments: Node N9. Both the formaldehyde molecules show the carbonyl moiety interacting with a 6c and a 5c site of the Pd cluster (O−Pd^{5c} 2.09 Å, C−Pd^{6c} 2.15 Å). This binding mode is very similar to that characterizing the interaction geometry of a single CH_2O molecule adsorbed on a smooth Pd(111) surface, as reported by Lim et al. (O−Pd 2.11 Å, C−Pd 2.15 Å).[42] Considering the molecular geometry of the CH_2O couple as a reasonable descriptor of lateral interactions, it is possible to argue that the coadsorbed CH_2O fragments slightly influence each other. The cleavage of the first C−H bond to form a CHO species, N10($CH_2O|CHO$), requires the overcoming of an activation barrier of 43.2 kJ mol^{-1}. The structural rearrangements occurring during the dehydrogenation do not affect the binding mode of the other CH_2O molecule placed on the Pd cluster, confirming as not influential the lateral interactions. The bond between the formyl species and the Pd cluster is characterized by two different bonds: one C−Pd in a bridge arrangement (C−Pd^{4c} 2.03 Å, C−Pd^{6c} 2.03 Å) and one atop O−Pd (O−Pd^{5c} 2.20 Å).

CH_2O + CHO Fragments: Node N10. The second consecutive C−H rupture shows an activation barrier of 9.9 kJ mol^{-1} and produces a coadsorbed CO molecule, N11-($CH_2O|CO$). According to Lim et al.[42] a formaldehyde H abstraction on a Pd(111) surface requires an activation barrier of ca. 38 kJ mol^{-1} while the dehydrogenation of the formyl species of ca. 60 kJ mol^{-1}. The findings here presented would suggest an opposite behavior; however, it is hard to state if this has to be related to the Pd cluster size or to other more subtle reasons.

CH_2O + CO Fragments: Node N11. The CH_2O dehydrogenation to initially produce a CHO species coadsorbed with a carbon monoxide molecule already present on the palladium cluster, N16(CHO|CO), and then a second coadsorbed CO molecule, N26(CO|CO), were analyzed, finding the related activation barriers 40.4 and 13.2 kJ mol^{-1}, respectively.

CHOCHO Species: Node N12. As glyoxal is a symmetric molecule, only one C−H and one C−C bond breaking process was analyzed. Their activation barriers were 64.7 and 75.7 kJ mol^{-1} for producing either N14−OOCCgC or two CHO fragments coadsorbed on the cluster, N15(CHO|CHO), respectively. The N14−OOCCgC species shows a terminal CO moiety bridging a 5c and a 6c site (C−Pd^{5c} 2.10 Å, C−Pd^{6c} 2.14 Å). On the contrary, the interaction geometry of the adsorbed formyl fragment is very similar to that previously reported for the decomposition of formaldehyde. Considering the values of the activation barriers calculated for these two molecular events, both the produced intermediates were further considered in the analysis.

$COCH_2O$ Species: Node N13. The analysis of the N13−OOCC reactivity would require the investigation of both a decarbonylation process and of a C−H bond cleavage. The latter, however, was not evaluated for two main reasons: due to the $COCH_2O$ surface arrangement (i) any among its C−H bonds was close enough to the cluster to be cleaved and (ii) the strong interaction with the metal sites did not allow any easy molecular rearrangements. The minimum amount of energy to form CO and formaldehyde coadsorbed on the Pd cluster, N11($CH_2O|CO$), starting from N13−OOCC was just 24.3 kJ mol^{-1}.

CHOCO Species: Node N14. Starting from N14−OOCCgC, the C−C and C−H bond cleavages were investigated. The C−C breaking, i.e., the decarbonylation process, showed an activation barrier of 28.2 kJ mol^{-1} whereas the C−H hydrogen abstraction 68.8 kJ mol^{-1}. The former transformation produces CO coadsorbed with CHO, N16(CHO|CO), whereas the latter, the dehydrogenated N25−OOCCgCC fragment.

$CHOCH_2OH$ Species: Node N4. For glycolaldehyde (N4−OC1), four molecular events were considered, namely C−H2, C−H1, C−C and O−H breaking (for the numbering of the hydrogen atoms, see Figure 4). The first three processes generating the species N17−OC1C2, N18−OC1C1 and N19($CH_2OH|CHO$) showed activation barrier values equal to 45.7, 84.1, and 122.8 kJ mol^{-1}, respectively. The O−H scission can take place only if changes in the glycolaldehyde interactions with the cluster occur because its local config-uration does not allow any interaction of the hydroxyl hydrogen atom with the metallic sites. This is likely due to the presence of an intramolecular hydrogen bond and to the structural rigidity caused by the carbonyl fragment interactions with the Pd cluster. The hydroxyl oxygen atom repositioning, from 6c to 5c site is on the other hand, a process requiring the overcoming of 26.2 kJ mol^{-1} and giving a product essentially iso-energetic with the starting species. The new configuration of glycolaldehyde on Pd_{12} shows the correct position for determining the O−H bond breaking, which actually occurs with an energy barrier equal to 73.4 kJ mol^{-1}. The intermediate obtained, N8−OOC*, however, cannot undergo the C−H2 scission, since both its H atoms point outward the cluster. An additional diffusion process must be thus invoked. This shows an activation barrier of 31.8 kJ mol^{-1} and converts N8−OOC* into N8−OOC. According to the activation barriers, further decomposition processes were investigated for the N17−OC1C2 intermediate and the connection between glycolaldehyde and the N8−OOC species, through a combined concurrence of diffusion steps and dehydrogenation, was considered as feasible.

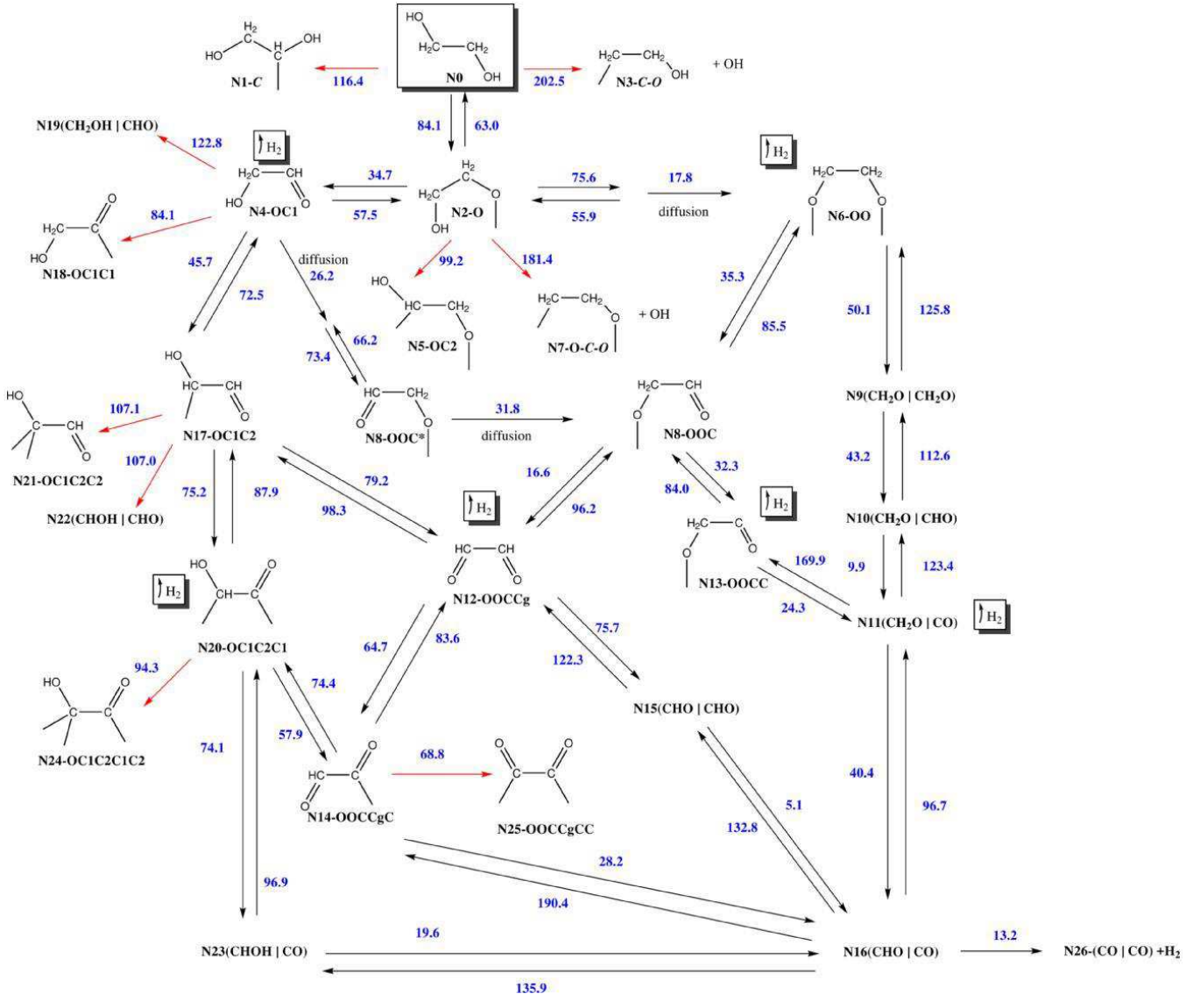

Figure 5. Whole decomposition mechanism of CH_2OH-CH_2OH to CO and H_2: points where one hydrogen molecule is assumed to leave the cluster are shown in squares; red arrows indicate pathways excluded during the presieving phase; energy barriers (expressed in kJ mol^{-1}) for bond scissions, formation and diffusions, in blue, refers to the reactant transformation. Dangling lines indicate bonds between fragments and Pd sites; interactions of chemically saturated atoms with the cluster are not shown.

CHOCHOH Species: Node N17. The intermediate produced from the C−H2 bond cleavage, N17−OC1C2, could be further decomposed by breaking C−H1, C−H2, C−C, and O−H bonds. The produced surface species and activation barriers are N20−OC1C2C1, N21−OC1C2C2, N22(CHOH|CHO), and N12−OOCCg and 75.2, 107.1, 107.0, and 79.2 kJ mol^{-1}, respectively. In agreement with the values of the activation barriers found, only the conversion of N17−OC1C2 either into N20−OC1C2C1 or N12−OOCCg was further considered.

COCHOH and CO + CHOH Species: Node N20 and N23. The N20−OC1C2C1 intermediate can undergo three different bond breaking events, namely C−H2, C−C, and O−H, that lead to two new intermediates N24−OC1C2C1C2, N23(CO| CHOH) and the already found N14−OOCCgC species. The related processes are characterized by activation barriers equal to 94.3, 74.1, and 57.9 kJ mol^{-1}. Because of these values, just the reactions leading to N23(CO|CHOH) and to N14− OOCCgC should be practicable. Furthermore, the N23(CO| CHOH) through dehydrogenation could be converted into the already met N16(CHO|CO) fragment, overcoming an activation barrier of 19.6 kJ mol^{-1}.

Reaction Network Analysis. The reaction mechanism for the CH_2OH-CH_2OH decomposition is reported in Figure 5. The C−O bond breaking seems to be, in any case, an energy demanding process, suggesting that Pd_{12} is not active in the alkane formation. The O−H bond scission shows an activation barrier between 70 and 80 kJ mol^{-1}, and is likely to occur in the early stages of the decomposition process; this indicates a tendency of the Pd_{12} cluster to be selective toward the formation of carbonylic, instead of enolic, compounds. These findings are confirmed by Griffin et al.[40] through HREELS and TPD studies, pointing out that formation and transformation of glyoxal are among the main processes involved in the CH_2OH-CH_2OH decomposition on Pd(111) planes. The C−H bond shows very different scission energy barriers, namely in the range 10−110 kJ mol^{-1}, and it is a process that has the chance to occur at every step along the C_2 species decomposition. The activation barrier in the C−C bond

cleavage usually decreases with decreasing the hydrogenation degree of the involved species; this phenomenon is increased if decarbonylation occurred. In agreement, comparing the C−C cleavage in N13−OOCC and N12−OOCCg, both having the same hydrogenation degree but involving and not involving decarbonylation activation barriers equal to 24.3 and 75.7 kJ mol^{-1} were found. Activation barrier of 28.2 kJ mol^{-1} was also found for N14−OOCCgC when decarbonylated.

Once obtained the whole reaction network, the trends associated with the variation of the spin states characterizing the systems during the reforming processes were analyzed. The multiplicity of the system could change for the elementary steps composing the ethylene glycol decomposition; however, the energy differences associated with the three analyzed spin states, i.e., triplet, quintet, and septet, generally resulted but with some remarkable exceptions in being small and, as a consequence, the emerging picture is too complex to be described by simple schemata. Still, some recurrent patterns for the surface species multiplicity variations as a function of the chemisorbed hydrogen quota on the Pd_{12} cluster could be found.

In Table 1 are reported all the intermediates species, related to the number of chemisorbed hydrogens on the cluster. For sake of clarity, at first, it is useful to analyze the species, whose C−C bond had not yet been broken: (i) apart from a few cases, species where the cluster is not hydrogenated showed more stable septet states than either quintet or triplet ones, which is in agreement with the most stable septet state of naked Pd_{12};
(ii) there are eight singly hydrogenated cluster systems and in most cases showed quintet as the most stable spin state, which is in agreement with the results of D'Anna et al.[31] showing a lowering of two units in the spin multiplicity when a dehydrogenation process occurs on a fragment in which the C−C bond is not yet cleaved; (iii) seven species with two chemisorbed hydrogens were analyzed, not showing a clear trend, so different spin states seem indeed to be favored. However, excluding N6−OO, having spin states very close in energy, the septet state is by far the less stable.

When the C−C bond is cleaved different coadsorbed unsaturated fragments on the cluster are formed, very likely inducing a spin state change of the systems. No simple trends, anyway, emerge by analyzing the results obtained for these species. However, when the C−C bond is cleaved, irrespective of the number of hydrogen atoms adsorbed on the Pd cluster, clearly it comes into view that triplet and quintet states are close in energy, being the former usually more stable than the latter, at variance with the septet that is less stable.

On the whole, 25 intermediates were characterized and thirty-one molecular events analyzed, resulting the final graph formed by 22 edges and 17 nodes. The intermediates omitted in the final graph are showed in Figure 5 as products of elementary steps pointed by red arrows while the connected undirected graph of the considered species is reported in Figure 6a.

There are several analyses that could be applied in order to extract information on the relevance of the nodes in a graph and, among these, the ones calculating the centrality indexes in GT are able to provide a node rank, identifying the most relevant in a considered context. Betweenness centrality (b−c), in particular, is representative of the node centrality in a given network. Here was calculated, by using the Brandes algorithm,[43] as implemented in the Gephi program.[44] The metric of the b−c parameter is defined by the number of shortest paths from any vertex to all the others, which cross a given node. A large b−c of a node actually indicates a substantial influence of it on the item transfer ability through the network. Therefore, when framed within a chemical context, even without energetic information, b−c could help to identify preliminarly key intermediates own of a reaction mechanism on the grounds of the solely connections between intermediates. The b−c of a given node, n, is

Table 1. Ethylene Glycol Decomposition Species in Absence (0H) or in the Presence of One (1H) or Two (2H) Co-Adsorbed Hydrogen Atoms on the Cluster[a]

	E(2S + 1) (kJ mol^{-1})		
0H	3	5	7
N0	22.5	9.1	0.0
N3−C−O	10.5	0.0	1.2
N4−OC1	73.0	42.0	0.0
N5−OC2	16.9	4.7	0.0
N6−OO	18.0	6.7	0.0
N12−OOCCg	17.5	7.3	0.0
N13−OOCC	20.2	10.2	0.0
N20−OC1C2C1	10.7	0.0	11.2
N21−OC1C2C2	41.9	0.0	35.3
N25−OOCCgCC	9.8	0.0	3.8
N9(CH_2O|CH_2O)	12.7	0.0	9.8
N11(CH_2O|CO)	9.4	0.0	46.9
N15(CHO|CHO)	6.7	0.0	41.7
N19(CH_2OH|CHO)	10.2	0.0	37.8
N23(CO|CHOH)	1.6	0.0	31.0
N26(CO|CO)	0.0	5.6	39.3
	E(2S + 1) (kJ mol^{-1})		
1H	3	5	7
N1−C	11.2	0.0	5.8
N2−O	17.6	6.8	0.0
N8−OOC	25.7	15.9	0.0
N14−OOCCgC	8.4	0.0	36.1
N17−OC1C2	11.8	0.0	18.2
N18−OC1C1	17.5	0.0	18.8
N24−OC1C2C1C2	0.0	3.5	83.2
N10(CH_2O|CHO)	0.0	6.1	32.9
N16(CO|CHO)	0.0	8.0	71.6
N22(CHOH|CHO)	0.0	2.0	39.5
	E(2S + 1) (kJ mol^{-1})		
2H	3	5	7
N4−OC1	13.1	0.0	32.1
N5−OC2	0.0	0.0	8.9
N6-OO	16.6	8.1	0.0
N12−OOCCg	5.2	0.0	34.8
N13−OOCC	4.3	0.0	28.8
N20−OC1C2C1	0.0	6.7	55.9
N21−OC1C2C2	0.0	17.5	58.9
N25−OOCCgCC[b]	−	0.0	51.5
N11(CH_2O|CO)	0.0	8.0	71.6
N26(CO|CO)	0.0	8.2	43.0

[a]For each species the energy difference E(2S+1) between triplet, quintet and septet state is reported. [b]The energy difference of the triplet state of N25−OOCCgCC is not reported because, irrespective of the initial guess, the system evolves into two separated CO molecules.

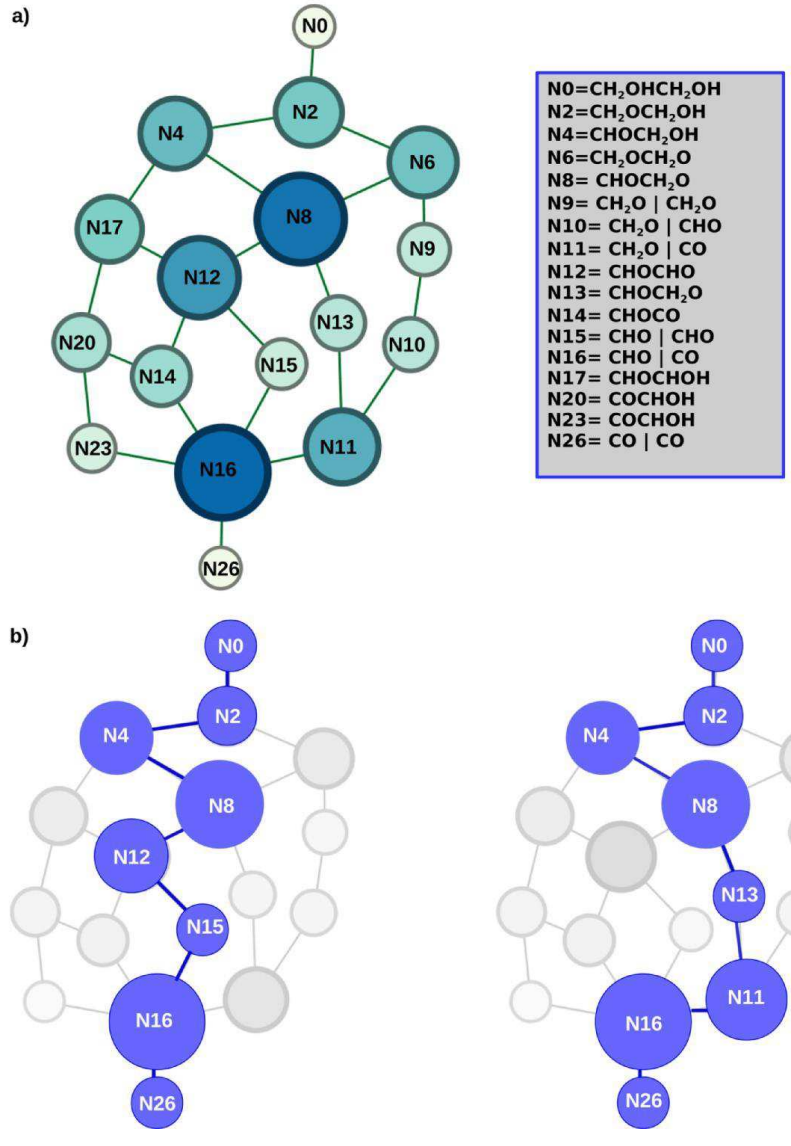

Figure 6. (a) Connected undirected graph of the reaction network: node size and color-gradient, from gray to blue, are related to the node betweenness centrality values. (b) Paths with the lowest TEC. Nodes are here individuated just by the first part of the species name.

$$b\text{-}c(n) = \sum_{s \neq n \neq t} \frac{\sigma st(n)}{\sigma_{st}} \quad (1)$$

with σ_{st} and $\sigma_{st}(n)$ being the number of paths linking, for the shortest route, nodes s and t and the ones, among these, that cross n.

In Figure 6, nodes are differently sized, according to their b− c values. From the connections properties of the nodes, it is evident that N8−OOC and N12−OOCCg are key intermediates of the title process, once more showing that glyoxal is fundamental in the ethylene glycol decomposition mechanism. Moreover, as already pointed out, 41 simple paths were found: 11 composed by 7 elementary steps as well as 14, 6, 8, and 2 with lengths 9, 11, 13, and 15, respectively (see Supporting Information).

These paths plainly represent the possible sequences of edges that connect the source node to the target one, without any energetic implication. In particular, in the title chemical framework, these are, nothing but, all the possible routes, given the intermediate set, to produce carbon monoxide starting from ethylene glycol. In the hypothesis that the total energy content could be used as an occurrence discriminating factor, characterizing different pathways, the latter were ordered by TEC values. The seven-cardinality sequences N0−N2−N4− N8−N12−N15−N16-N26 and N0−N2−N4−N8−N13− N11−N16-N26, as reported in Figure 6b, following the inference above, should be the most probable. These routes both includes glycolaldehyde and the N8−OOC species. In the former, the glyoxal formation is followed by the C−C bond cleavage that would occur after its formation, again suggesting a kind of selectivity to the carbonylic compounds by the here considered Pd_{12} cluster. Instead in the second path, the C−C bond scission will occur by means of the N13−OOCC intermediate decarbonylation.

CONCLUSIONS

Reaction networks are complex systems often composed by several interconnecting routes. In the present study various ethylene glycol, CH_2OH-CH_2OH, decomposition pathways occurring on a subnanometric Pd_{12} cluster were characterized by means of density functional theory calculations, aimed at pinpointing the energy of reagents, products, and intermediates

as well as transition states linking them. A starting presieving phase, based on the analysis of elementary step activation barrier values, allowed us to exclude several molecular events because highly unprobable, hence to delineate a peculiar selectivity of the Pd_{12} to the carbonylic intermediate formation, keeping completely out the enolic formation possibility. A graph theory, GT, based analysis, applied on events of comparable activation energies, allowed us to individuate the possible pathways starting from CH_2OH-CH_2OH and leading to H_2 and CO. Glycolaldehyde and glyoxal seem to be cornerstones of the whole reaction mechanism while the C−C cleavage likely occurs only after the formation of scarcely hydrogenated intermediates. It was finally noted that GT centrality indexes, outlining the role of nodes within graphs, could be of interest also in the analysis of the tangled reaction mechanism.

ASSOCIATED CONTENT

* Supporting Information

The Supporting Information is available free of charge on the ACS Publications website at DOI: 10.1021/acs.jpcc.7b00850.

Reaction paths potentially taking place, along with the ethylene glycol decomposition calculated by means of GT, optimized Cartesian coordinates of intermediates, and transition states characterizing the reaction network along with the energy and imaginary frequency of transition states (PDF)

AUTHOR INFORMATION

Corresponding Author

*(D.Du.) E-mail: dario.duca@unipa.it. Telephone: +39-091-23897975. Fax: +39-091-23860815.

ORCID

Remedios Cortese: 0000-0002-7232-8916
Roberto Schimmenti: 0000-0003-1129-2988
Francesco Ferrante: 0000-0002-2989-4365
Antonio Prestianni: 0000-0002-4631-7121

Notes

The authors declare no competing financial interest.

ACKNOWLEDGMENTS

Funding is gratefully acknowledged by European Union Seventh Framework Programme (FP7/2007−2013) within the project SusFuelCat “Sustainable fuel production by aqueous phase reforming−understanding catalysis and hydrothermal stability of carbon supported noble metals” GA: CP-IP 310490 (http://cordis.europa.eu/projects/rcn/106702_en.html).

REFERENCES

(1) Cortright, R. D.; Davda, R. R.; Dumesic, J. A. Hydrogen from Catalytic Reforming of Biomass-derived Hydrocarbons in Liquid Water. Nature 2002, 418, 964−967.

(2) Huber, G. W.; Cortright, R. D.; Dumesic, J. A. Renewable Alkanes by Aqueous-Phase Reforming of Biomass-Derived Oxygen-ates. Angew. Chem., Int. Ed. 2004, 43, 1549−1551.

(3) Deluga, G. A.; Salge, J. R.; Schmidt, L. D.; Verykios, X. E. Renewable Hydrogen from Ethanol by Autothermal Reforming. Science 2004, 303, 993−997.

(4) Alonso, D. M.; Bond, J. Q.; Dumesic, J. A. Catalytic Conversion of Biomass to Biofuels. Green Chem. 2010, 12, 1493−1513.

(5) Sutton, J. E.; Panagiotopoulou, P.; Verykios, X. E.; Vlachos, D. G. Combined DFT, Microkinetic, and Experimental Study of Ethanol Steam Reforming on Pt. J. Phys. Chem. C 2013, 117, 4691−4706.

(6) Kirilin, A. V.; et al. Aqueous-Phase Reforming of Xylitol over Pt/ C and Pt/TiC-CDC Catalysts: Catalyst Characterization and Catalytic Performance. Catal. Sci. Technol. 2014, 4, 387−401.

(7) McManus, J. R.; Salciccioli, M.; Yu, W.; Vlachos, D. G.; Chen, J. G.; Vohs, J. M. Correlating the Surface Chemistry of C_2 and C_3 Aldoses with a C_6 Sugar: Reaction of Glucose, Glyceraldehyde, and Glycolaldehyde on Pd(111). J. Phys. Chem. C 2012, 116, 18891− 18898.

(8) Medlin, J. W. Understanding and Controlling Reactivity of Unsatured Oxygenates and Polyols on Metal Catalysts. ACS Catal. 2011, 1, 1284−1297.

(9) Xiong, K.; Yu, W.; Vlachos, D. G.; Chen, J. G. Reaction Pathways of Biomass-Derived Oxygenates over Metals and Carbides: From Model Surfaces to Supported Catalysts. ChemCatChem 2015, 7, 1402−1421.

(10) Zaffran, J.; Michel, C.; Auneau, F.; Delbecq, F.; Sautet, P. Linear Energy Relations As Predictive Tools for Polyalcohol Catalytic Reactivity. ACS Catal. 2014, 4, 464−468.

(11) Davis, J. L.; Barteau, M. A. Decarbonylation and Decomposition Pathways of Alcohols on Palladium (111). Surf. Sci. 1987, 187, 387− 406.

(12) Davis, J. L.; Barteau, M. A. The Influence of Oxygen on the Selectivity of Alcohol Conversion on the Palladium (111) Surface. Surf. Sci. 1988, 197, 123−152.

(13) Davis, J. L.; Barteau, M. A. Spectroscopic Identification of Alkoxide, Aldehyde, and Acyl Intermediates in Alcohol Decomposition on Palladium (111). Surf. Sci. 1990, 235, 235−248.

(14) Jiang, R.; Guo, W.; Li, M.; Fu, D.; Shan, H. Density Functional Investigation of Methanol Dehydrogenation on Pd(111). J. Phys. Chem. C 2009, 113, 4188−4197.

(15) Ferrin, P.; Simonetti, D.; Kandoi, S.; Kunkes, E.; Dumesic, J. A.; Nørskov, J. K.; Mavrikakis, M. Modeling Ethanol Decomposition on Transition Metals: A Combined Application of Scaling and Brønsted-Evans-Polanyi Relations. J. Am. Chem. Soc. 2009, 131, 5809−5815.

(16) Prestianni, A.; Crespo-Quesada, M.; Cortese, R.; Ferrante, F.; Kiwi-Minsker, L.; Duca, D. Structure Sensitivity of 2-Methyl-3-butyn-2-ol Hydrogenation on Pd: Computational and Experimental Modeling. J. Phys. Chem. C 2014, 118, 3119−3128.

(17) Cortese, R.; Schimmenti, R.; Armata, N.; Ferrante, F.; Prestianni, A.; Duca, D.; Murzin, D. Y. Investigation of Polyol Adsorption on Ru, Pd, and Re Using vdW Density Functionals. J. Phys. Chem. C 2015, 119, 17182−17192.

(18) Crespo-Quesada, M.; Yoon, S.; Jin, M.; Prestianni, A.; Cortese, R.; Cardenas-Lizana, F.; Duca, D.; Weidenkaff, A.; Kiwi-Minsker, L. Shape-Dependence of Pd Nanocrystal Carburization during Acetylene Hydrogenation. J. Phys. Chem. C 2015, 119, 1101−1107.

(19) Prestianni, A.; Cortese, R.; Ferrante, F.; Schimmenti, R.; Duca, D.; Hermans, S.; Murzin, D. Y. α-d-Glucopyranose Adsorption on a Pd_{30} Cluster Supported on Boron Nitride Nanotube. Top. Catal. 2016, 59, 1178−1184.

(20) Shekhar, R.; Barteau, M. A. Structure Sensitivity of Alcohol Reactions on (110) and (111) Palladium Surfaces. Catal. Lett. 1995, 31, 221−237.

(21) Christmann, K.; Demuth, J. E. The Adsorption and Reaction of Methanol on Pd(100). I. Chemisorption and Condensation. J. Chem. Phys. 1982, 76, 6308−6317.

(22) Zanchet, D.; Santos, J. B. O.; Damyanova, S. J.; Gallo, M. R.; Bueno, J. M. C. Toward Understanding Metal-Catalyzed Ethanol Reforming. ACS Catal. 2015, 5, 3841−3863.

(23) Li, M.; Guo, W.; Jiang, R.; Zhao, L.; Shan, H. Decomposition of Ethanol on Pd(111): A Density Functional Theory Study. Langmuir 2010, 26, 1879−1888.

(24) Yudanov, I. V.; Matveev, A. V.; Neyman, K. M.; R osch, N. How the C−O Bond Breaks during Methanol Decomposition on Nanocrystallites of Palladium Catalysts. J. Am. Chem. Soc. 2008, 130, 9342−9352.

(25) Sutton, J. E.; Vlachos, D. G. Ethanol Activation on Closed-Packed Surfaces. Ind. Eng. Chem. Res. 2015, 54, 4213−4225.
(26) Lei, Y.; et al. Increased Silver Activity for Direct Propylene Epoxidation via Subnanometer Size Effects. Science 2010, 328, 224− 228.
(27) Lee, S.; et al. Oxidative Decomposition of Methanol on Subnanometer Palladium Clusters: The Effect of Catalyst Size and Support Composition. J. Phys. Chem. C 2010, 114, 10342−10348.
(28) Mehmood, F.; Greeley, J. P.; Curtiss, L. A. Density Functional Studies of Methanol Decomposition on Subnanometer Pd Clusters. J. Phys. Chem. C 2009, 113, 21789−21796.
(29) Frisch, M. J.; et al. Gaussian 09, Revision C.01; Gaussian Inc.: Wallingford, CT, 2009.
(30) Zhao, Y.; Truhlar, D. A new Local Density Functional for Main-group Thermochemistry, Transition Metal Bonding, Thermochemical Kinetics, and Noncovalent Interactions. J. Chem. Phys. 2006, 125, 194101−194110.
(31) D'Anna, V.; Duca, D.; Ferrante, F.; La Manna, G. DFT Studies on Catalytic Properties of Isolated and Carbon Nanotube Supported Pd_9 Cluster-I: Adsorption, Fragmentation and Diffusion of Hydrogen. Phys. Chem. Chem. Phys. 2009, 11, 4077−4080.
(32) Barone, G.; Duca, D.; Ferrante, F.; La Manna, G. CASSCF/CASPT2 Analysis of the Fragmentation of H_2 on a Pd_4 Cluster. Int. J. Quantum Chem. 2010, 110, 558−562.
(33) Duca, D.; Ferrante, F.; La Manna, G. Theoretical Study of Palladium Cluster Structures on Carbonaceous Supports. J. Phys. Chem. C 2007, 111, 5402−5409.
(34) D'Anna, V.; Duca, D.; Ferrante, F.; La Manna, G. DFT Studies on Catalytic Properties of Isolated and Carbon Nanotube Supported Pd_9 cluster. Part II. Hydro-isomerization of Butene Isomers. Phys. Chem. Chem. Phys. 2010, 12, 1323−1328.
(35) Ferrante, F.; Duca, A. P. D.; et al. Computational Investigation of Alkynols and Alkyndiols Hydrogenation on a Palladium Cluster. J. Phys. Chem. C 2014, 118, 551−558.
(36) Howard, D. L.; Jørgensen, P.; Kjaergaard, H. G. Weak Intramolecular Interactions in Ethylene Glycol Identified by Vapor Phase OH-Stretching Overtone Spectroscopy. J. Am. Chem. Soc. 2005, 127, 17096−17103.
(37) Das, P.; Das, K. P.; Arunan, E. Conformational Stability and Intramolecular Hydrogen Bonding in 1,2-ethanediol. J. Phys. Chem. A 2015, 119, 3710−3720.
(38) Mavrikakis, M.; Barteau, M. A. Oxygenate Reaction Pathways on Transition Metal Surfaces. J. Mol. Catal. A: Chem. 1998, 131, 135−147.
(39) Schimmenti, R.; Cortese, R.; Duca, D.; Mavrikakis, M. Boron Nitride-supported Sub-nanometer Pd_6 Clusters for Formic Acid Decomposition: A DFT Study. ChemCatChem 2017, 9, 1610.
(40) Griffin, M. B.; Jorgensen, E. L.; Medlin, J. W. The Adsorption and Reaction of Ethylene Glycol and 1,2-Propanediol on Pd(111): A TPD and HREELS Study. Surf. Sci. 2010, 604, 1558−1564.
(41) Scaranto, J.; Mavrikakis, M. HCOOH Decomposition on Pt(111): A DFT study. Surf. Sci. 2016, 650, 111−120.
(42) Lim, K. H.; Chen, Z.; Neyman, K. M.; Rösch, N. Comparative Theoretical Study of Formaldehyde Decomposition on PdZn, Cu, and Pd Surfaces. J. Phys. Chem. B 2006, 110, 14890−14897.
(43) Brandes, U. A Faster Algorithm for Betweenness Centrality. J. Math. Sociol. 2001, 25, 163−177.
(44) Bastian, M.; Heymann, S.; Jacomy, M. Gephi: An Open Source Software for Exploring and Manipulating Networks; 2009.